Nano Energy, Volume 33, March 2017, Pages 146-156
DOI:10.1016/j.nanoen.2017.01.037

Flexible piezoelectric nano-composite films for kinetic energy harvesting from textiles

Ahmed Almusallam[a], Zhenhua Luo[b], Abiodun Komolafe[a], Kai Yang[a], Andrew Robinson[c], Russel Torah[a] and Steve Beeby[a]*

[a] Department of Electronics and Computer Science (ECS), University of Southampton, Southampton, SO17 1BJ, UK
[b] School of Water, Energy and Environment, Cranfield University, College Road, Cranfield, MK43 0AL, UK
[c] Faculty of Engineering and the Environment, University of Southampton, Southampton, SO17 1BJ, UK
* Corresponding author

Abstract. This paper details the enhancements in the dielectric and piezoelectric properties of a low-temperature screen-printable piezoelectric nano-composite film on flexible plastic and textile substrates. These enhancements involved adding silver nano particles to the nano-composite material and using an additional cold isostatic pressing (CIP) post-processing procedure. These developments have resulted in a 18% increase in the free-standing piezoelectric charge coefficient d_{33} to a value of 98 pC/N. The increase in the dielectric constant of the piezoelectric film has, however, resulted in a decrease in the peak output voltage of the composite film. The potential for this material to be used to harvest mechanical energy from a variety of textiles under compressive and bending forces has been evaluated theoretically and experimentally. The maximum energy density of the enhanced piezoelectric material under 800 N compressive force was found to be 34 J/m^3 on a Kermel textile. The maximum energy density of the enhanced piezoelectric material under bending was found to be 14.3 J/m^3 on a cotton textile. These results agree very favourably with the theoretical predictions. For a 10 cm x 10 cm piezoelectric element 100 μm thick this equates to 38 μJ and 14.3 μJ of energy generated per mechanical action respectively which is a potentially useful amount of energy.

Keywords
Piezoelectric, nano-composite, energy harvesting, textiles, screen printed

1. Introduction

Electronic textiles (e-textiles) are a form of wearable technology that has the potential to revolutionise the wearable technology sector. E-textile solutions face the same challenge as with all wearable devices, namely that of supplying electrical power. At present the only solution is to use batteries and whilst this suits rigid wearable devices, they are less compatible with flexible textiles and the requirement to periodically charge the battery is an ongoing inconvenience. Energy harvesting potentially provides an alternative power source that could replace or augment a battery solution. This paper explores the potential of a flexible piezoelectric film screen printed onto a textile for harvesting mechanical energy from the textile and converting it into electrical energy [1-3]. One application of such an approach would be to harvest the kinetic energy present in human movement that would cause clothing fabric to flex and compress. The compressive and bending forces would be transferred to the piezoelectric film enabling the mechanical to electrical energy transduction process to occur. Piezoelectric transduction is a very widely used method for harvesting mechanical energy and many example devices have been published including cantilever based structures with bonded bulk [4] and screen printed [5] lead zirconate titanate (PZT). More recently, nano-scale materials have been explored such as ZnO nanowires [6] and BaTiO3 nanofibres aligned within a flexible polydimethylsiloxane (PDMS) matrix [7].

To be used in such an application, the piezoelectric materials needs to be flexible thereby minimising its effect on the feel of the textile and the user's comfort. The common piezoelectric materials, such as PZT ceramics, possess excellent dielectric and piezoelectric properties but are physically hard and brittle and are inherently unsuitable for such an application. Alternative polymer piezoelectric materials, such as polyvinylidenefluride (PVDF) and associated co-polymers, are flexible and can be cured at low temperature, which is suitable for use with fabrics. PVDF yarns have also been woven into a textile [8] but the typical piezoelectric coefficients e.g. d_{33} are an order of magnitude lower than ceramic PZT being

in the range of 13 to 38 pC/N [9]. This results in lower energy conversion efficiency and limits the power output of the energy harvester.

This paper investigates the use of a screen printable piezoelectric composite to form an active film on the surface of the textile for energy harvesting. Formulated correctly, it offers the potential for improved piezoelectric properties compared with PVDF as well as a suitable degree of flexibility provided by the polymer binder. The most common and most straightforward to formulate piezoelectric composite is the 0-3 type which contains piezoelectric ceramic powder dispersed in a polymer or epoxy binder [10, 11]. The 0-3 type piezoelectric composites can be deposited on to a substrate using a number of techniques, but this work used screen-printing since it is a straightforward and scalable process that is widely used in the textile industry.

The piezoelectric response of a piezoelectric composite is typically affected by a reduction in the effective electric field (E_{eff}) during the poling process [12]. This is caused by the lower dielectric constant and higher resistivity of the polymer phase of the composite compared to the ceramic phase, which traps the applied electric field within the polymer matrix, and the E_{eff} applied across the piezoelectric particle is reduced. E_{eff} can also be reduced by air voids within the composite introduced during mixing of the composite, or during the curing process when the solvent is evaporated. These air voids also reduce the overall dielectric constant and increase the resistivity of the film, consequently reducing the E_{eff} on the piezoelectric particles.

To minimize the reduction in E_{eff}, in this work we report on an investigation into the addition of silver nano-particles into the polymer matrix. Adding conductive particles into the composite can significantly lower the resistivity of the polymer phase [13], thus increasing the E_{eff} on the piezoelectric particles. Previous studies have investigated a number of additives in piezoelectric composite, such as carbon nanotubes [14], micron-sized Ag particles [15], and Ag nanowires [16]. This work used nano-sized Ag particles (average size of 100 nm) in the composite.

This paper builds upon previously published investigations into the formulation of a low temperature screen printable piezoelectric composite carried out at Southampton. This work takes the previously best performing formulation [17] and reports on the effect of adding different amounts of Ag nano particles on the film properties. The work also uses cold isostatic press (CIP) post-processing, which was previously found to reduce the air voids in the composite [18]. The improved piezoelectric composite ink has been printed on 4 types of flexible substrates (Kapton, cotton, polyester cotton and Kermel) and the energy harvesting potential of this approach has been evaluated both theoretically and experimentally. Characterizing equations and experiments are presented that apply to the printed films under compressive and bending forces. The influence of the mechanical properties of the flexible substrates on the energy harvesting performance are also explored since this has previously been demonstrated to have an effect on the measured d_{33} or the printed films [19].

2. Materials and Methods

2.1 Formulating piezoelectric composite paste

In this work, a mixture of piezoelectric ceramic particles and polymeric binder was used to make the piezoelectric composite paste. The polymeric binder was formed by mixing a thermoplastic polymer with γ-butyrolactone solvent to produce a thixotropic paste. Lead zircontate titanante (PZT) piezoelectric ceramic powder, type PZT-5H was used as the active material in the composite. The ceramic powder was a blend of PZT particles with an average particle size of 2 μm (Pz29, Ferroperm) and 0.8 μm (S-55, Sunnytec) with weight ratio of 4:1. This blend PZT powder sizes has been previously identified as a suitable combination form maximizing the density of the piezoelectric particles with the smaller particles filling the voids between the larger particles [17]. The PZT powder mixture was blended with the polymeric binder in a weight ratio of 2.57:1, making a printable paste.

The Ag nanoparticles with an average particle size of 100 nm (Sigma Aldrich) were added to the paste. The dielectric and piezoelectric properties of the printable paste were investigated for different Ag weight

percentages of 0.05, 0.1, 0.2, 0.5, 1 and 2, respectively. The mixture was first hand mixed using spatula and then placed in a DAC 150 SpeedMixer (Synergy Device Limited) for 2 minutes. The mixtures were finally processed in a triple-roll mill (Exact 501) to further improve the PZT and Ag powder dispersion and to minimize trapped air in the dispersion. A schematic of the formulation process is shown in figure 1(a).

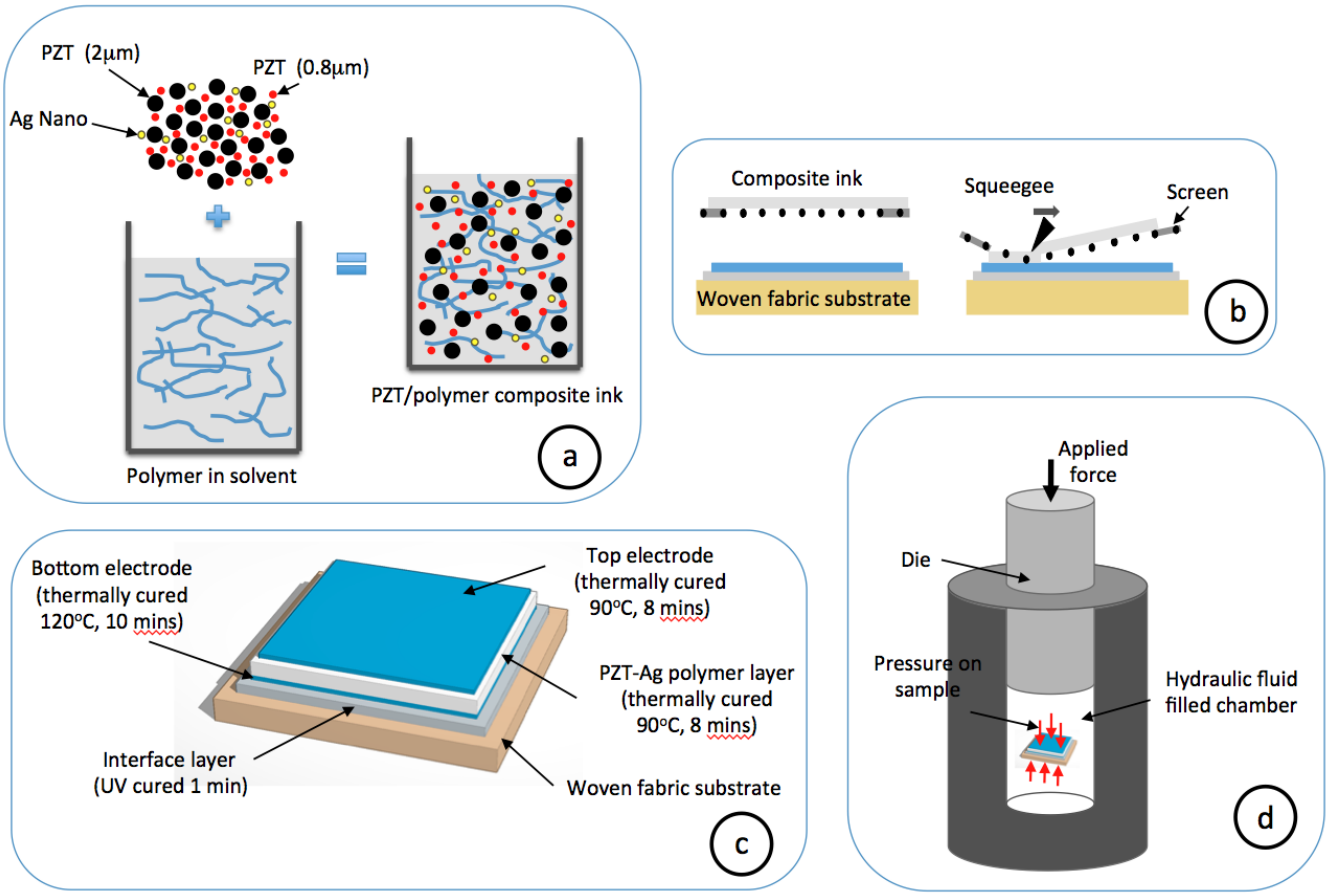

Figure 1: Schematic showing (a) the mixing process of the PZT-Ag-polymer composite; (b) the screen printing process; (c) the printed capacitive structure on woven-fabric substrate; (d) the CIP process.

2.2 Screen-printing and curing the piezoelectric paste

The piezoelectric material and other associated layers were screen-printed using a DEK 248 semi-automatic screen-printer (DEK Printing Machines Ltd) and stainless steel mesh screens (see figure 1(b)). The piezoelectric composite was printed in a standard parallel plate capacitor structure with the piezoelectric film sandwiched between two electrodes as shown in figure 1(c). This capacitor structure enables contact poling of the piezoelectric material and straightforward connection to the electrodes for the measurement of d_{33} and in actual use. The screen-printing process was carried out on. In the case of textiles, it is often necessary to first print a polymer interface layer on the surface of the fabric before printing the other layers. This interface layer reduces the surface roughness and negates any surface pilosity (protruding fibres) that would otherwise prevent the printing of consistent working samples [20]. The interface layer is a UV curable polyurethane based paste (Fabink-UV-IF1, Smart Fabric Inks). The remaining films were all thermally cured in a box over, with the curing conditions of each printed layer being shown in figure 1(c). The electrodes were printed using silver polymer ink from DuPont (DuPont 5000). The dimensions of the printed samples used in this study were 10 x 10 mm by approximately 100 μm thick.

2.3 Poling process

Direct contact poling (DCP) was used to polarize the piezoelectric active particles in the composite. An external electric field (E, MV/m) was applied for a specific period of time (t, min) with the sample held at an elevated temperature (T, °C). E is defined by the equation E = V/d, where V and d are the applied voltage and the thickness of the composite film, respectively. Throughout this study, the external electric field used was 3.7 MV/m and the poling time was 6 minutes. The poling temperature varied between 70 and 90 ^{o}C depending upon the formulation and the exact values T for the different formulations and the influence of the additives and post processes are discussed in the text below.

2.4 Cold isostatic pressing (CIP)

A commercial CIP machine (CIP-15, MTI Corporation USA) was used to eliminate the air voids in the printed piezoelectric film. As schematically shown in figure 1(d), the vertical applied force on the die pressurizes the hydraulic fluid inside the vessel, resulting in a homogenous pressure that is applied to the sample. This increases the density of the composite phases (PZT, Ag particles and polymer) and reduces the air voids. An Scanning Electron Microscope (SEM) image of the top of the cured and pressed piezoelectric film is shown in figure 2.

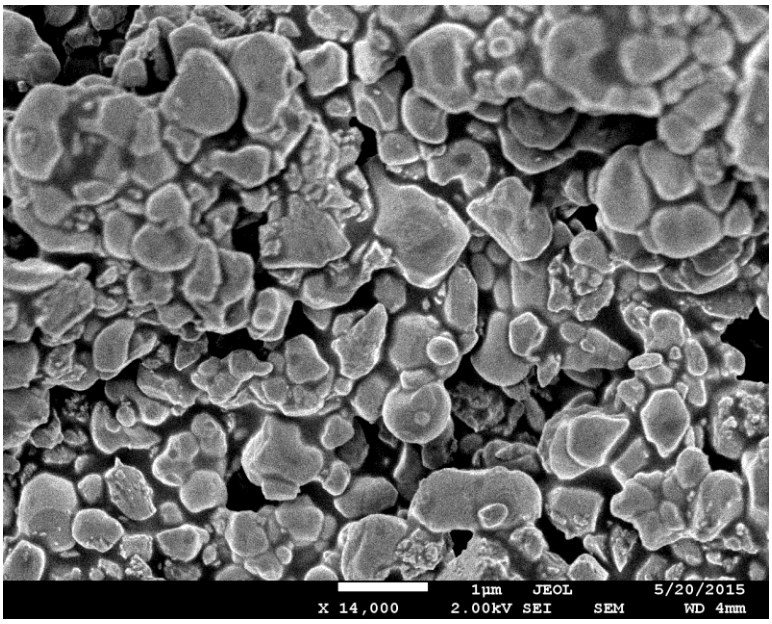

Figure 2: SEM image of the cured and pressed piezoelectric layer

2.5 Flexible substrates

The paste was screen-printed on two types of substrates, Kapton polyimide 300HN (75 µm, KATCO) and woven-fabrics. The Kapton substrate is mainly used as a reference for investigating the dielectric and piezoelectric properties of the composite. The piezoelectric composite on woven-fabric substrates is the main focus in this study. The outputs (voltage, power and energy) of the printed composite on the woven-fabric substrates were measured under compressive and bending forces. The investigated woven-fabric substrates were polyester-cotton (65% polyester), cotton, and polyamide-imide (Kermel). Table 1 lists the Young's modules (Y_f) and Poisson ratio (v) of the fabrics, interface layer and deposited films. The effective Young's modulus and Poisson ratio of each composite were calculated using the following equations.

$$Y_{sub} = Y_f . V_f + Y_{int} . V_{int} \qquad (1)$$

$$\upsilon_{sub} = \upsilon_f . V_f + \upsilon_{int} . V_{int} \qquad (2)$$

Where, Y_{sub}, υ_{sub}, Y_f, υ_f, Y_{int}, and υ_{int} are the Young's modulus and Poisson ratio of the substrate, fabrics and interface layer, respectively. Since the volume fraction of the interface layer for cotton, polyester-cotton and Kermel substrates are 0.7, 0.7 and 0.4 respectively, the Young's modulus and Poisson ratio of the substrates were estimated and are given in Table 2. The values in Table 2 were used to calculate the theoretical voltage output of the composite in the following section.

Table 1: Mechanical properties of substrates and the piezoelectric film

Material	Direction	Young's modulus (MPa)	Average Poisson ratio ν
Cotton	Warp	505	0.5
	Weft	415	
Polyester-cotton	Warp	534	0.42
	Weft	356	
Kermel	Warp	247	0.38
	Weft	244	
Interface layer	-	100	0.47
Kapton	-	2500	0.34
Piezoelectric film	-	131	0.4

Table 2: Mechanical properties of the substrates (woven-fabric plus interface)

Woven-fabric plus interface layer	Y (MPa)	υ
Cotton	352	0.491
Polyester-cotton	342	0.435
Kermel	158	0.434

3. Analytical modelling of energy output

The piezoelectric composite is modelled as a unimorph piezo-beam under compressive and bending conditions. Due to the mechanical behaviour of fabrics under these loads, the elastic properties of the fabrics were characterized based on [21] to improve the correlation between the experimental and theoretical results. The energy outputs of the composite due to compressive and bending stresses are characterised as follows:

(a) Compressive case

The voltage ouput of the piezoelectric composite on woven-fabric substartes can be predicted using analytical modelling. The following three constitutive equations describe the mechanical and electrical behaviour of the piezoelectric element and these use the standard subscript notation to describe the vector directions.

$$S_1 = s_{11}^E T_1 + s_{12}^E T_3 + d_{31} E_3 \quad (3)$$

$$S_3 = s_{13}^E (T_1 + T_2) + s_{33}^E T_3 + d_{33} E_3 \quad (4)$$

$$D_3 = \varepsilon_3^T E_3 + d_{31} (T_1 + T_2) + d_{33} T_3 \quad (5)$$

where, S, T, E and D are the strain, stress (N/m^2), electric field (MV/m), and electric displacement (C/m^2), respectively. In addition, s, d and ε represent the mechanical compliance (m^2/N), piezoelectric coefficient (C/N) and the dielectric constant, respectively.

When placed on an isotropic substrate (the fabric plus interface layer), the lateral strain is the same in each direction $S_1=S_2$ and the stress $T= T_1=T_2$, equation (5) can be re-written as

$$D_3 = \varepsilon_3^T E_3 + 2d_{31}T + d_{33}T_3 \qquad (6)$$

Also, at open circuit conditions: $D_3=0$, therefore equation (6) can be derived into

$$-\varepsilon_3^T E_3 = 2d_{31}T + d_{33}T_3 \qquad (7)$$

Thus, the value of S_1 and S_2 must be determined as a function of T_3 using Hooke's law

$$S_1 = S_2 = \left(-\frac{\nu_{sub}}{Y_{sub}}\right)T_3 \qquad (8)$$

Relating the strain and the ratio of the generated charge to the applied force and combining with equations (3) (4) and (8) gives

$$-\left(\frac{\nu_{sub}}{Y_{sub}}\right)T_3 = (s_{11}^E + s_{12}^E)T + s_{13}^E T_3 + d_{31}E_3 \qquad (9)$$

To simplify the equation, we express $A = s_{11}^E + s_{12}^E$ and $B = \frac{\nu_{sub}}{Y_{sub}}$, equation (7) becomes

$$T = \frac{-s_{13}^E T_3 - d_{31}E_3 - BT_3}{A} \qquad (10)$$

Substituting (10) into (7)

$$E_3 = \frac{Ad_{33} - 2d_{31}s_{13}^E - 2d_{31}B}{2d_{31}^2 - A\varepsilon_3^T}T_3 \qquad (11)$$

then,

$$\frac{V_{oc}}{t_p} = \frac{Ad_{33} - 2d_{31}s_{13}^E - 2d_{31}B}{2d_{31}^2 - A\varepsilon_3^T}T_3 \qquad (12)$$

then,

$$V_{oc} = \frac{(s_{11}^E + s_{12}^E)d_{33} - 2d_{31}s_{13}^E - 2d_{31}\left(\frac{\nu_{sub}}{Y_{sub}}\right)}{2d_{31}^2 - (s_{11}^E + s_{12}^E)\varepsilon_3^T}.t_p.T_3 \qquad (13)$$

From Hooke's law, assuming the piezoelectric composite film is isotropic, the relationship between d_{33} and d_{31} is

$$d_{31} = \nu_p.d_{33} \qquad (14)$$

By substituting equation (14) in equation (13), Equation (15) can be derived.

$$V_{oc} = \frac{(s_{11}^E + s_{12}^E).d_{33} - 2v_p.d_{33}.s_{13}^E - 2v_p.d_{33}.\left(\frac{v_{sub}}{Y_{sub}}\right)}{2.\left(v_p.d_{33}\right)^2 - (s_{11}^E + s_{12}^E).\varepsilon_3^T}.t_p.T_3 \quad (15)$$

Equation (15) includes the mechanical factor from the substrates to calculate the output voltage. It helps to predict the output voltage of piezoelectric films on different substrates. This mechanical factor is expressed as $\left(\frac{v_{sub}}{Y_{sub}}\right)$ in Equation (15). The type of the force applied (bending or compressive) can be represented by the stress T_3 in the equation. When under compressive force, the stress component T_3 can be calculated by $T_3=F_3/A_e$, where F_3 is the force applied in 3-direction and A_e is the effective area.

(b) Bending case

In bending, however, T_3 becomes the bending stress on the piezoelectric layer. Two different models that calculate the bending stress on the piezoelectric films were compared in this work. These are based on the Stoney's equation [22] and classical beam theory (CBT) [21].

Stoney's equation for calculating stress on a film is shown in Equation (16). It assumes that the thickness of the substrates and piezoelectric layer are negligibly small when compared to the bending radius of the composite structure [22].

$$\sigma_f = \frac{Y_{sub}\, h_{sub}^2 r}{6h_f(1 - v_{sub})} \quad (16)$$

where σ_f and h_f are the stress and thickness of the film, respectively. In this model, $\sigma_f = T_3$, thus Equation (16) can be substituted into Equation (15) to calculate the output voltage of the piezoelectric film in bending.

The bending stress on any layer of a multilayer composite based on CBT is given by [21]:

$$T_3 = \sigma_i = Y_i \epsilon_i = \frac{Y_i \left(\sum_{j=1}^{i} h_j - \bar{y}\right)}{r} \quad (17)$$

where σ_i, Y_i, ϵ_i and h_i are the bending stress, elastic modulus, strain and thickness of the i^{th} layer in the composite, while $\bar{y}$ and r are the neutral axis and the bending radius of the composite, respectively.

The neutral axis of the multilayer piezoelectric beam of uniform width is obtained using [23]:

$$\bar{y} = \frac{\sum_{i=1}^{n} Y_i h_i \left(2\sum_{j=1}^{i} h_j - h_i\right)}{2\sum_{i=1}^{n} Y_i h_i} \quad (18)$$

In fabric-substrated multilayer composites, the different elastic modulus of the fabric substrates in tension and compression is critical to determining the value of $\bar{y}$. Hence, in bending, the fabric substrate can be treated as a two-layer material with one layer under tensile force, and the other layer under compressive force. These two layers with thicknesses h_1 and h_2 are separated by the neutral axis. They are characterized by the compressive and tensile moduli, Y_C and Y_T of the fabric, respectively. The value of h_1 and h_2 are defined as follows [19]:

$$h_1 = \bar{y}_{fabric} \quad (19)$$
$$h_2 = h_{fabric} - \bar{y}_{fabric}$$

where, $\bar{y}_{fabric}$ and h_{fabric} are the neutral axis and thickness of the fabric. Hence, in the model using CBT, the value of T_3 in Equation (17) can be obtained using the neutral axis in Equation (18), and then used to calculate the output voltage of the piezoelectric film with Equation (15).

4. Results and Discussion

The results are divided into two parts. The first part relates to the improvements made to the piezoelectric composite material whilst the second part reports the evaluation of the energy harvesting potential from textiles using the improved piezoelectric material.

4.1 Dielectric and piezoelectric properties of the PZT-Ag-polymer nano-composite

Piezoelectric composites with Ag wt% of 0%, 0.05%, 0.1%, 0.2%, 0.5% and 1% were investigated. These were screen-printed on to Kapton substrates and cured as described previously. Their dielectric properties are shown in figure 3(a). The results show that the relative dielectric constant increases and then decreases with increasing % weight content of Ag nano-particles with 0.2 wt% giving a dielectric constant of 171. A similar trend to the relative dielectric constant is observed in the d_{33}, as shown in figure 3(b). The d_{33} of the composite reaches a maximum value of 43.5 pC/N at 0.2 wt% of Ag in the composite, showing an 8% increase compared to the composite without Ag. The d_{33} was found to decrease beyond 0.2 wt%. It should be noted that the poling temperature used varies with Ag wt%, being 90°C for 0%, 80°C for 0.05 and 0.1% and 75°C for 0.2 and 0.5%. The increasing Ag content was found to increase the risk of short-circuiting during poling, which can be countered by reducing the poling temperature.

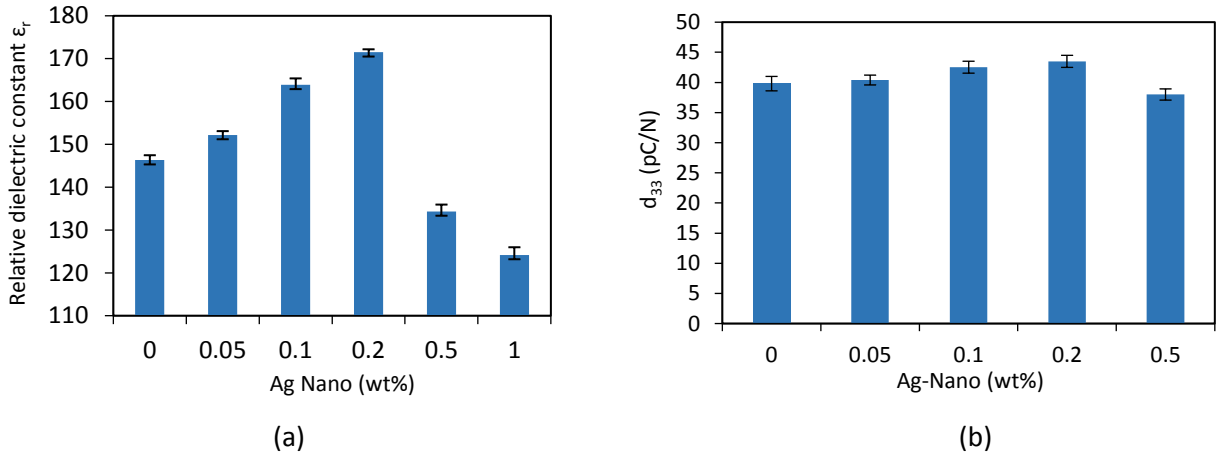

Figure 3 (a) Relative dielectric constant of the composite measured at 1 Hz, with increasing wt% of Ag nano-particles and (b) d_{33} value of the PZT-Ag-polymer composite with different Ag wt% (poling temperature reduces with increasing %Ag)

Different substrates have a different effect on the measured d_{33} values due to the clamping effect caused by the variation in mechanical boundary conditions of the substrates, which has been discussed in our previous work [19]. Taking the relative mechanical properties of the Kapton and polyester-cotton substrates into account and applying the theory presented in [19] then the 0.2 wt% Ag composite printed on a polyester-cotton substrate would exhibit a freestanding d_{33} value of 76 pC/N.

4.2 Effect of CIP pressure on the dielectric, resistive and piezoelectric properties

Composite samples on Kapton with 0.2 wt% Ag content were next processed at different CIP pressures and the relative dielectric constant, DC resistivity and piezoelectric properties of the samples measured. For each CIP pressure, three samples were tested. The dielectric constant was found to increase with

increasing CIP pressure, as shown in figure 4(a), whilst the DC resistivity decreases. The application of a CIP pressure of 250 MPa for 2 minutes was found to lead to a 44% increase in the dielectric constant and a decrease of 52.8% in the DC resistivity. The reduction in resistivity can cause breakdown at high electric fields during the polarization process. To offset this, the poling temperature was reduced to 70°C for the samples pressurized at 250 MPa. Figure 4(b) shows the effect of increasing CIP pressure on the d_{33} values. The samples pressurized by 250 MPa demonstrate a 9% increase in d_{33} compared to the samples with 0.2 wt% Ag but without CIP processing. Combined, the addition of the Ag nano particles and the use of CIP yields d_{33} of 49 pC/N on Kapton, an increase in the measured d_{33} of 9 pC/N compared to the original composite. All samples were poled at 75°C apart from the CIP pressure of 250 MPa, which was poled at 70°C to ensure reliable poling.

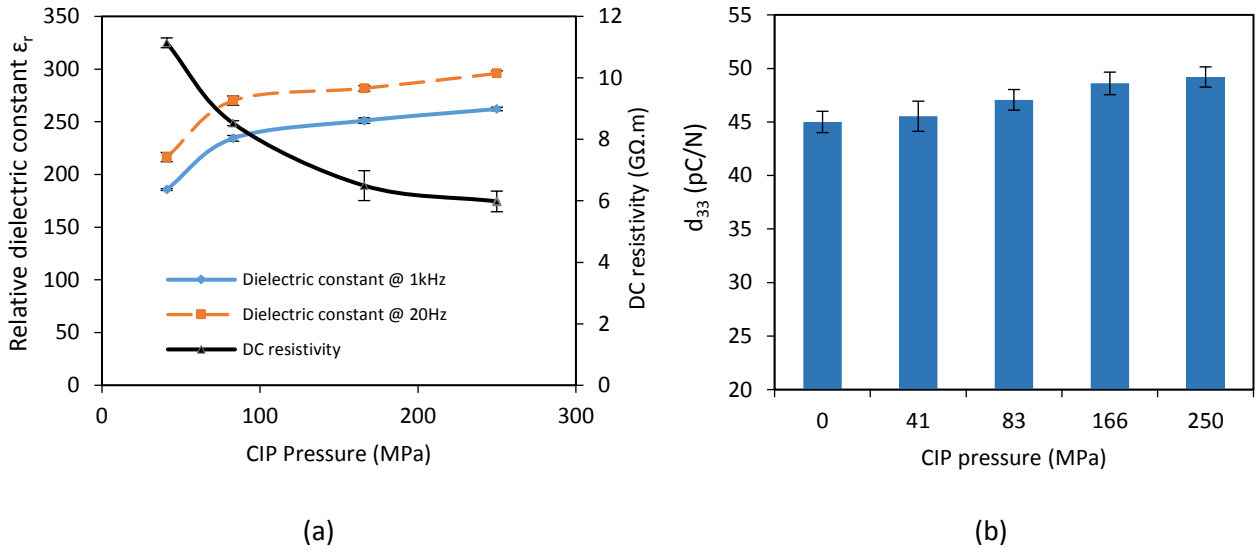

Figure 4 (a) Relative dielectric constant (at 20 Hz and 1 kHz) and DC resistivity of the samples with increasing CIP pressure and processing time of 2 mins and (b) d_{33} values of the samples processed at different CIP pressures.

Table 3 shows a summary of improvements in the dielectric, piezoelectric and resistive properties of the composite by adding Ag nano-particles and applying the CIP process compared with the original formulation. The summary includes the piezoelectric properties for films printed on Kapton, polyester-cotton (as an example of the woven-fabric substrate), and free-standing. The free-standing d_{33} value is calculated from the measured d_{33} value to determine the actual d_{33} if there was no substrate [19]. Table 4 give other mechanical properties of the original piezoelectric composite film.

Table 3: Summary of the improvement in the dielectric, piezoelectric and resistive properties

Sample type			**Kapton**		**Polyester-cotton**		**Free-standing**	
	ε_r (at 1 kHz)	R_v (GΩ.m)	d_{33} (pC/N)	g_{33} (mV.m/N)	d_{33} (pC/N)	g_{33} (mV.m/N)	d_{33} (pC/N)	g_{33} (mV.m/N)
Original	146	12.5	40	30.9	70	54.2	80	62
Original + CIP (250 MPa)	211	7.1	45	24	76.6	41	90	48.2
0.2 wt% Ag	171	11.7	43.5	28.7	76	50.2	87.5	57.8

0.2 wt% Ag + CIP (250 MPa)	262	5.9	49	21.1	83	35.8	98	42.2

Table 4: Mechanical properties of the piezoelectric film

Parameter	Value
Y_p (MPa)	131
υ_p	0.4
s_{11} (m^2/N)	7.63×10^{-9}
s_{12} (m^2/N)	-3.05×10^{-9}
s_{13} (m^2/N)	-3.05×10^{-9}

4.3 Energy harvesting from textiles from compressive force

In wearable energy harvesting application the most commonly used source of kinetic energy is from the compressive force generated by the heel strike during the gait cycle. This force was replicated and applied to the piezoelectric composite films printed on the different substrates using the compressive force profile shown in figure 5. This equates to an 81.5kg individual with a heel strike every second. The force was applied using an Instron ElectroPuls E1000 dynamic and fatigue testing system. The output voltages from the samples were recorded using a digital oscilloscope (TDS2014, Tekronix Ltd).

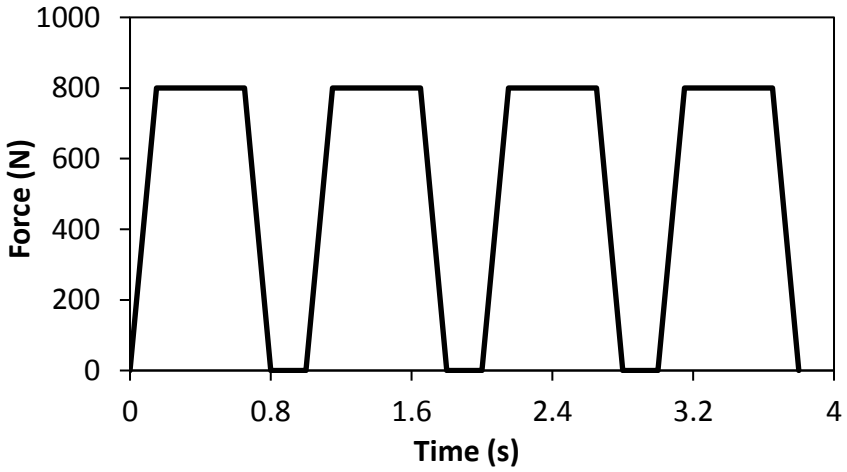

Figure 5: Applied compressive force profile.

(a) Effects of Ag nano-particles and CIP processing on the energy output in compression

The outputs of the both the original and improved piezoelectric composite materials have been evaluated. The peak output voltage (V_{peak}), peak power density (P_d) and energy density (E_d) were first obtained by applying compressive forces to polyester-cotton substrate samples. These values were measured at varying external resistive loads in the range of $1 \leq R_L \leq 80$ MΩ. Figure 6 shows that for both the original and 0.2 wt% Ag + CIP piezoelectric material, the peak voltage increases with increasing resistive load. The 0.2 wt% Ag + CIP material has lower peak voltage than the original. As the peak power density was calculated from the peak voltage using equation 20, the 0.2 wt% Ag + CIP material also shows lower power density with a maximum P_d of 160 W/m^3 at optimum resistive load of 40 MΩ. The original material gives a maximum P_d of 434 W/m^3 at optimum resistive load of 10 MΩ. The lower peak voltage

of the 0.2 wt% Ag + CIP piezoelectric material is due to its lower g_{33}, which is caused by the increased dielectric constant, as shown in Figures 3 and 4.

$$P_d = \frac{V_{peak}^2}{R_L} V_f \tag{20}$$

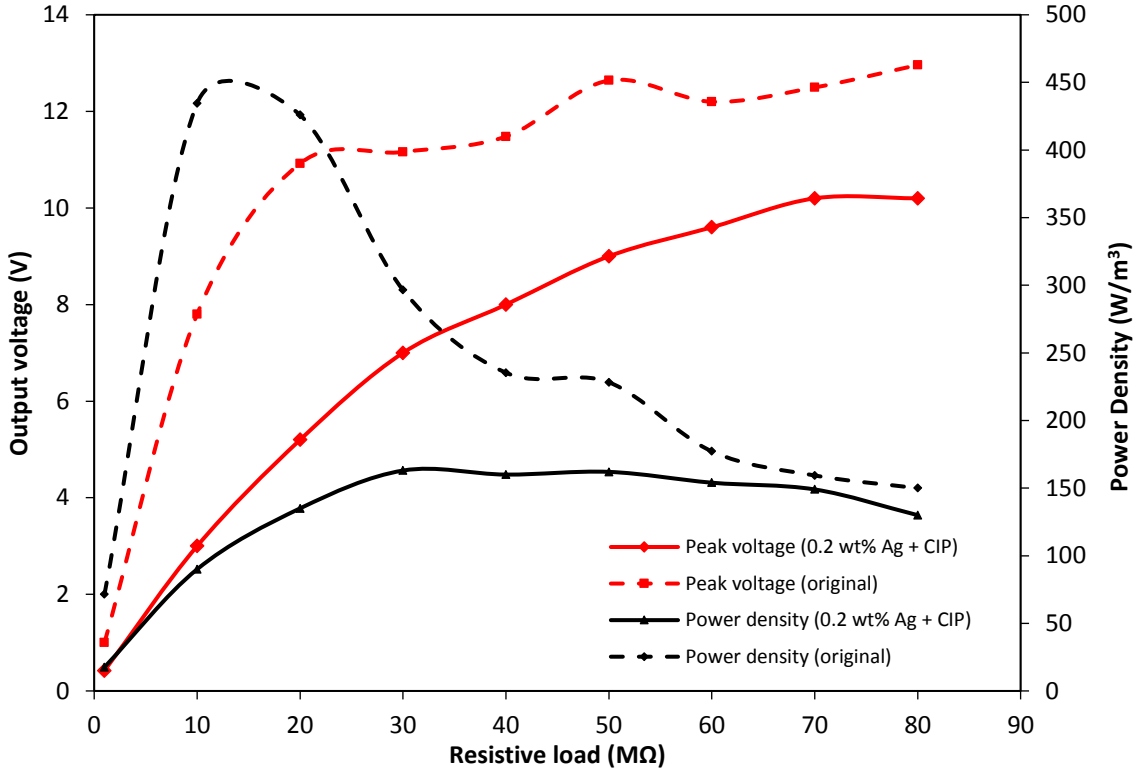

Figure 6: Output peak voltage and power density of the original and 0.2 wt% Ag + CIP materials on polyester-cotton under compression.

Figure 7 shows the variation in energy densities of the original and 0.2 wt% Ag + CIP composite materials with increasing the external resistive load. The energy density is calculated using the equation 21, where t_1 and t_2 represent the beginning and end time of the pulse generated by compressing the sample. The maximum energy density of the 0.2 wt% Ag + CIP composite is 24 J/m^3 at an optimum resistive load of 50 MΩ, and for the original composite is 12 J/m^3 at 20 MΩ. The increase in E_p is due to the increase of d_{33} in the improved composite materials and the longer duration of the pulse ($t_2 - t_1$) compared with the original material (see inset in figure 8). As shown in Table 3, d_{33} increases with increasing ε_r, leading to an overall increase in output energy.

$$E = V_f \int_{t_1}^{t_2} \frac{V(t)^2}{R} . dt \tag{21}$$

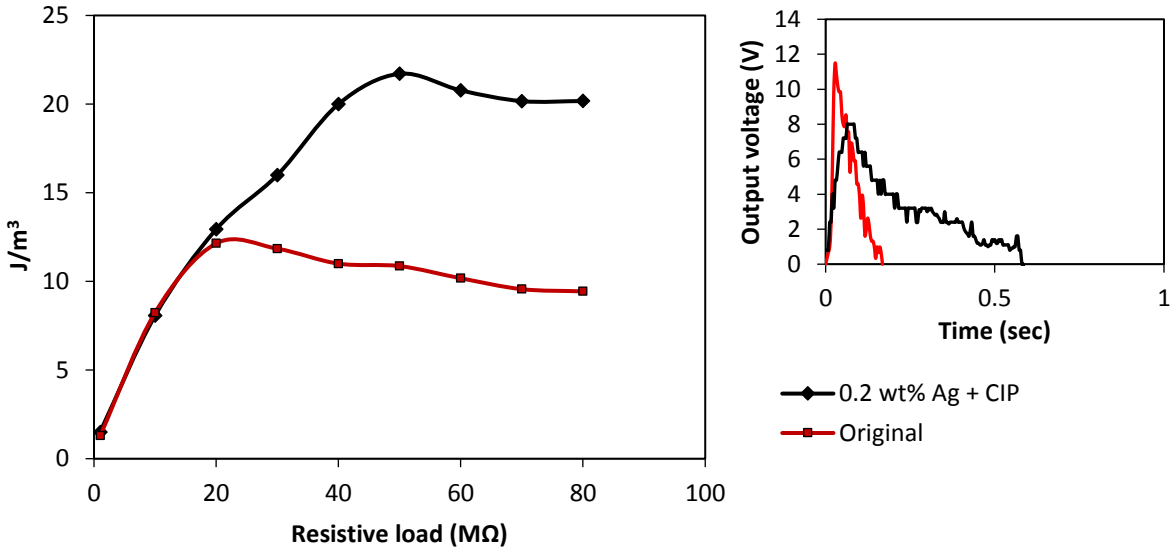

Figure 7: Energy density of samples on polyester-cotton of the original and 0.2 wt% Ag + CIP composites under 800 N compressive force. The inset shows the generated pulses at 40 MΩ.

Figure 8 shows the open-circuit voltage V_{Poc} and short-circuit current I_{Psc} of the 0.2 wt% Ag + CIP composite under 800 N of compressive force. The maximum values are 19 V and 0.54 µA respectively. These outputs compare favorably with other composite piezoelectric materials reported in the literature [24, 25].

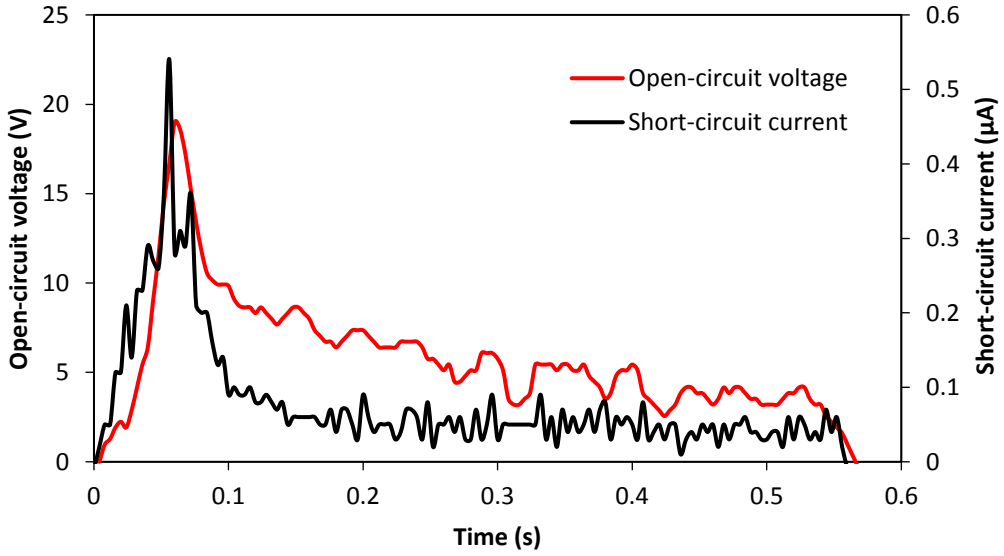

Figure 8: Open-circuit voltage V_{oc} and short-circuit current I_{sc} of the 0.2 wt% Ag + CIP composite on polyester-cotton under 800 N compressive force.

4.4 Effect of substrate on energy harvesting under compressive force

The influence of the different flexible substrates on the energy output from the 0.2 wt% Ag + CIP composite has been calculated using Equation 15 and obtained experimentally. Figure 9(a) shows the calculated and measured open-circuit voltages from 800 N compressive force for the Kapton, cotton, polyester-cotton and Kermel substrates. The substrates are placed in order of compliance from least

(Kapton) to most (Kermel) as detailed in tables 1 and 2. The experimental and calculated results both show that the open-circuit output voltage increases with increasing compliance of the substrates.

Figure 9(b) shows the energy densities of the 0.2 wt% Ag + CIP composite printed on the three woven-fabric substrates with varying external resistive loads. The results show that the maximum energy densities achieve peak values of 14, 22 and 34 J/m^3 at resistive load of 30, 50 and 50 MΩ for cotton, polyester-cotton and Kermel respectively. This result is related to the compliance of the substrate with the least compliant (cotton) demonstrating the lowest energy density and Kermel, which is most compliant substrate, producing the highest energy.

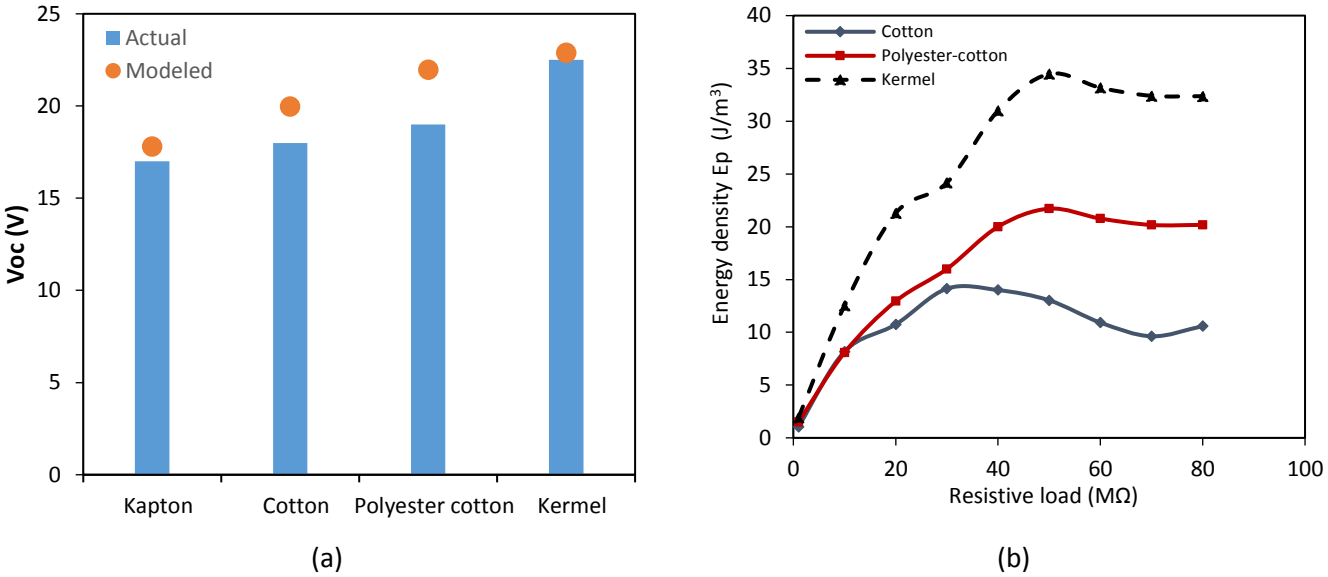

Figure 9 (a) Experimental and modelled open-circuit voltages of the of the 0.2 wt% Ag + CIP composite on different substrates when applying a compression force of 800 N and (b) energy densities of the 0.2 wt% Ag + CIP composite printed on cotton, polyester-cotton and Kermel substrates under 800 N of compressive force, with varying external resistive loads.

The difference in the output energy of the composite on cotton, polyester-cotton and Kermel substrates is due to the variation in the mechanical boundary conditions of the printed film. This is identical to the clamping effect of the substrate during the direct measurement of the d_{33} values of the films. The substrate clamps the film on its bottom surface and therefore the lateral movement of the films during loading is affected by the strain in the substrate. The compressive force in the 3-direction (through the film thickness) produces a lateral strain (S) in the 1-2 plane due to the Poisson's ratio. Due to the difference in the Poisson's ratio, the expansion of the film and substrate will be different and the substrate will strain the film in the 1-2 direction introducing a d_{31} component to the charge generated by the film. Since the d_{31} coefficient is of the opposite sign to the d_{33} coefficient, the charge generated is of the opposite sign and this reduces the net charge generated. The magnitude of the d_{31} charge component is determined by the compliance of the substrate with more compliant materials transferring less strain to the piezoelectric film. Therefore the lower the compliance of the fabric then the greater the net charge generated from the compressive force.

4.5 Energy harvesting from textiles from bending

The samples were subjected to bending force applied at a frequency of 1 Hz using the rig shown in figure 10(a). The bending force was applied at one end of the sample with the other end fixed, as shown in the schematic in figure 10(b), which replicates the testing procedure used in other works [26].

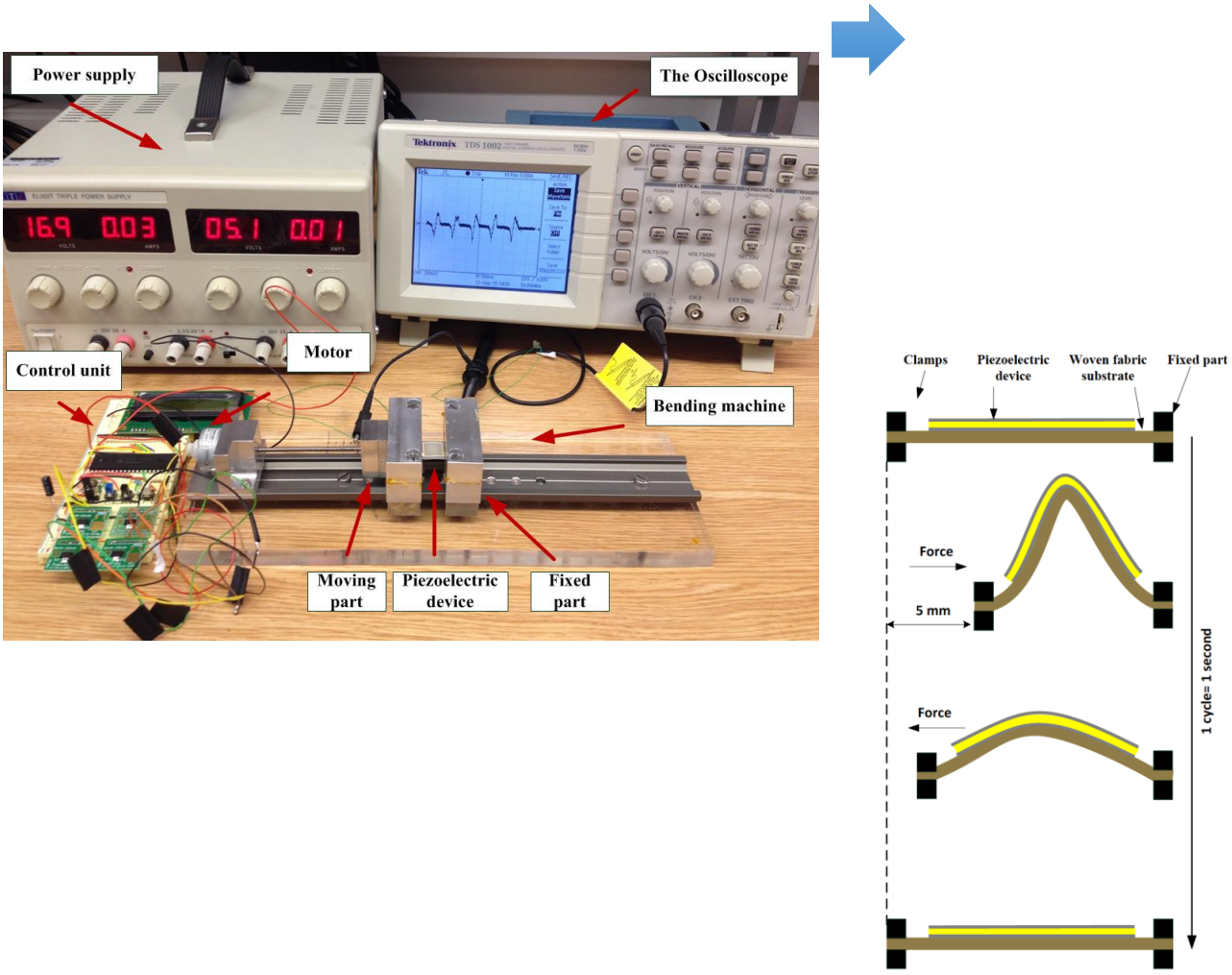

Figure 10: (a) The bending test rig and (b) schematic showing bending force applied to the test sample

(a) Effects of Ag nano-particles and CIP processing on the energy output in bending

Similar to the results from compression test, the peak voltage and power density of the 0.2 wt% Ag + CIP composite are lower than the original, as shown in Figure 11. This is again due to the lower g_{33} and higher d_{33} of the 0.2 wt% Ag + CIP material.

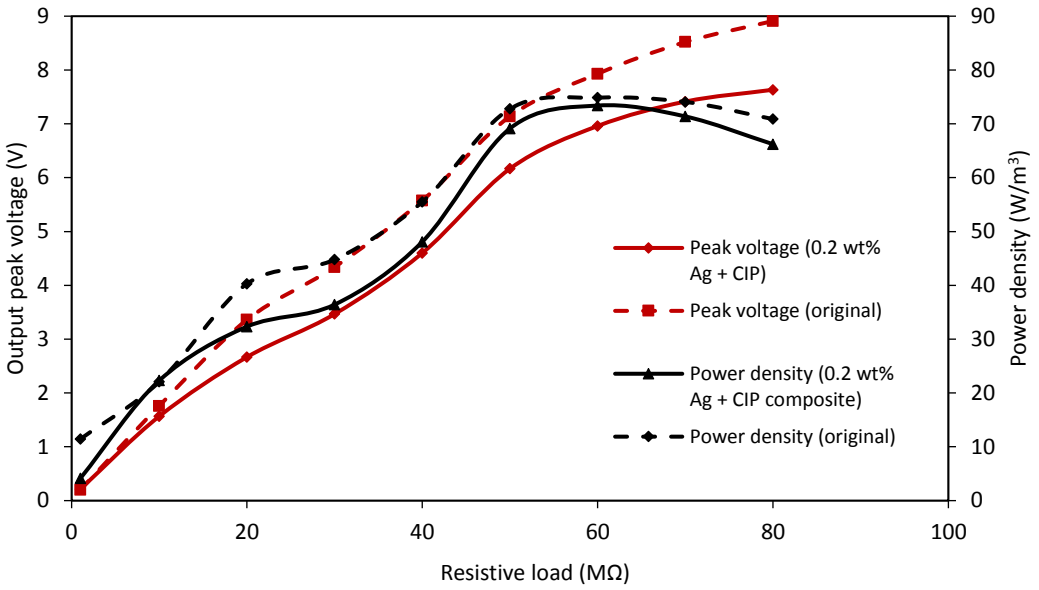

Figure 11: Output peak voltage and power density of the original and 0.2 wt% Ag + CIP composites under the same bending force. Polyester-cotton was used as substrate for both samples.

The 0.2 wt% Ag + CIP composite produced a maximum V_{Poc} of 17 V and maximum I_{Psc} of 0.34 µA, as shown in Figure 12. These values are higher than those previously reported [26].

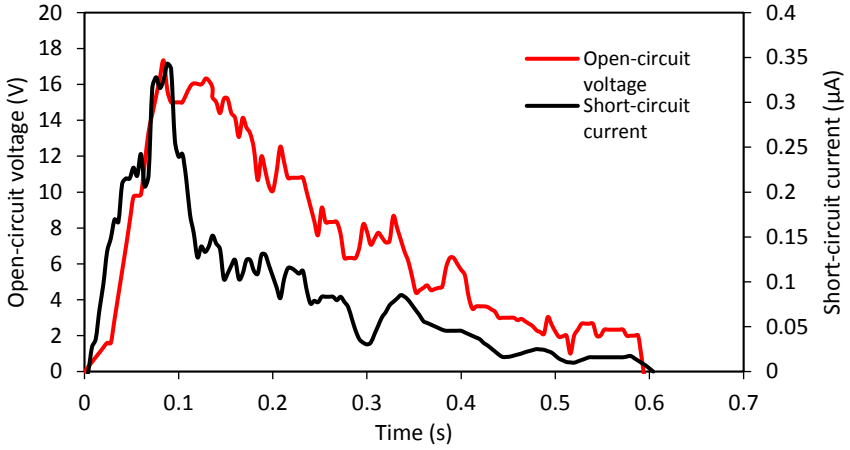

Figure 12: Open-circuit voltage V_{oc} and short-circuit current I_{sc} when applying bending force at 1 Hz on the 0.2 wt% Ag + CIP composite

Similar to the results of the compression test in figure 7, the 0.2 wt% Ag + CIP composite shows higher energy densities than the original material, as shown in figure 13. The processed sample shows a peak energy density of 12 J/m^3 at 50 MΩ, and the sample without processing shows peak energy density of 11 J/m^3 at 70 MΩ. This is due to the higher d_{33} of the processed film.

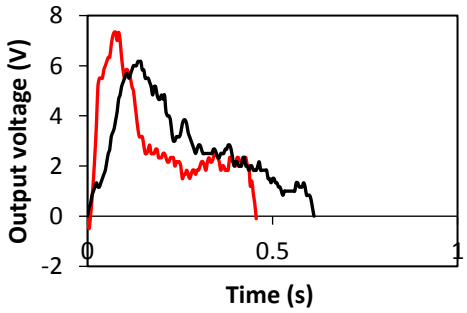

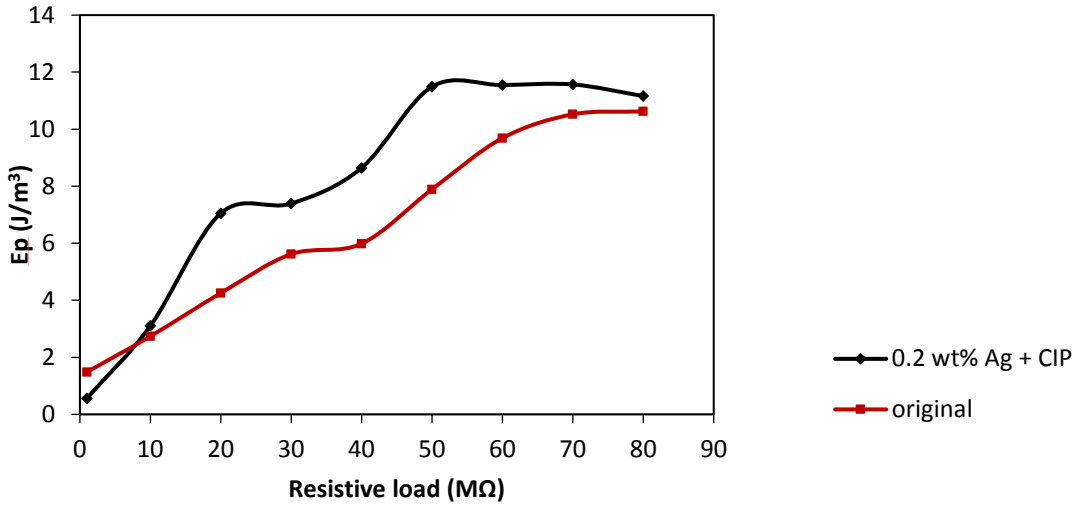

Figure 13: Energy density of samples on polyester-cotton of the original and 0.2 wt% Ag + CIP composites during bending. The inset shows the generated pulses at 50 MΩ.

(b) Effects of substrate on the energy output

Similar to the compression test, the output of the composite is also affected by the type of woven-fabric substrate in the bending test. However, when in compression the output is mainly affected by the mechanical boundary conditions of the substrates but the situation is more complex for the bending case. From the model presented previously, the radius of curvature, bending rigidity and the neutral axis of the system also affect the bending case. The voltage output calculated using Stoney's model and the model presented in this paper based on classical beam theory (CBT) are compared with experimental results in figure 14(a). The CBT based model includes the effect of the substrate (i.e. the bending radius and neutral axis) and is therefore more accurate than Stoney's model. Figure 14(b) compares the energy densities of the piezoelectric films on different fabric substrates. For the cotton, polyester-cotton and Kermel substrates, their energy densities reach peak values of 14.3, 11.5 and 11.6 J/m^3 at resistive loads of 70, 50 and 80 MΩ, respectively. It shows that cotton, which is least compliant among the three substrates, produced the highest energy density because its increased stiffness couples more strain into the piezoelectric composite film.

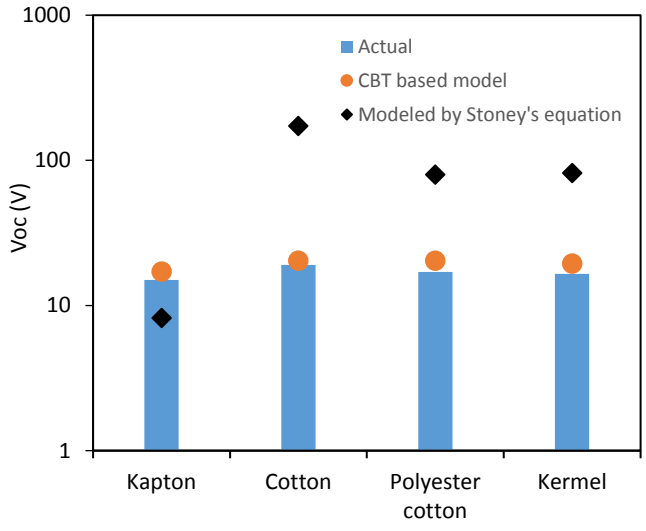

(a)

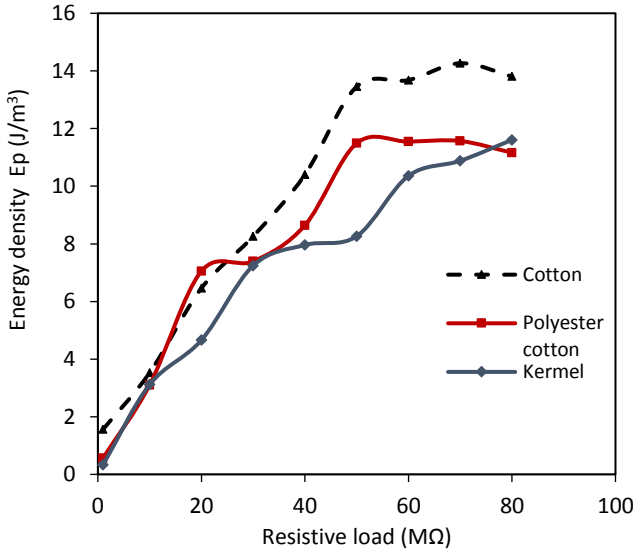

(b)

Figure 14 (a) Experimental and modeled open-circuit voltages of the 0.2 wt% Ag + CIP composite film on different woven-fabrics when applying a bending at 1 Hz and a radius of curvature of 0.6 cm and (b) energy densities of the 0.2 wt% Ag + CIP film printed on cotton, polyester-cotton and Kermel substrates when applying bending force at 1Hz, with varying external resistive loads.

6. Conclusions

This work investigates the energy harvesting performance of PZT-polymer composite materials printed on woven-fabric substrates. Clearly the energy harvesting performance is fundamentally linked to the piezoelectric properties of the printed film. Diluting piezoceramic powder by placing it in a polymer matrix will reduce the level of piezoelectric activity compared to bulk piezoceramic materials, but measures such as the addition of Ag nano-particles and applying cold isostatic pressing has improved performance. These measures have resulted in a 18% increase in the free-standing piezoelectric charge coefficient d_{33} of the printed composite. The evaluation of the energy harvesting performance of the improved piezoelectric composite printed on woven substrates has resulted in an increase in energy density of 200% and 10% in compression and bending respectively. The increased dielectric constant has led to a decrease in the piezoelectric voltage coefficient g_{33}, thus lowering the peak output voltage.

The comparison between the different woven substrates shows that the energy output from the printed piezoelectric composite is affected by the mechanical properties of the woven fabric. When placed in compression, the highest energy output was obtained on the fabric with the smallest Young's modulus, i.e. the most compliant. On the other hand, when flexed or bent, the highest energy output was obtained from the fabric with highest Young's modulus. The models presented in this paper to describe the energy output of the piezoelectric composite in compression and bending show good agreement with the experimental results and are useful tools for predicting the output from such materials in these applications.

For a 10 cm x 10 cm piezoelectric element 100 □m thick, the energy density results equate to 38 μJ and 14.3 μJ of energy generated per mechanical action respectively. Piezoelectric harvesters are typically fabricated on stiffer substrates such a metal or silicon and therefore other piezoelectric harvesters of similar size would typically deliver more energy especially in bending. The compliance of the textile substrates, which is a fundamentally desirable property for the comfort of the wearer, does reduce the strain coupled to the piezoelectric film and hence the level of energy generated. Nonetheless, the energy generated is a potentially useful amount and may be useful for powering wearable electronics in the future as the levels of power consumption continue to fall.

Acknowledgements

The authors gratefully acknowledge the EPSRC for supporting this research with grant reference EP/I005323/1. The data for this paper can be found at DOI:10.5258/SOTON/403388.

Bio's

Dr Ahmed Almusallam received the BS.c in electrical and computer engineering in 2006, the MS.c in Micro ElectroMechanical Systems (MEMS) from University of Southampton, United Kingdom, in 2010 and completed his Ph.D from University of Southampton, United Kingdom in 2016. His Ph.D research was to develop flexible piezoelectric nano-composite materials for energy harvesting from textiles. His research interests include energy harvesting (from various sources, e.g. vibration, human movement, solar and thermoelectric), flexible electronics, developing piezoelectric materials, sensors, e-textiles, nanofabrication, printed electronics and thick-film technology.

Dr Zhenhua Luo completed his PhD at University of New South Wales (Australia), focusing on the development and characterization of lead-free piezoelectric materials. During PhD he was awarded a fellowship and worked at Technical University Darmstadt (Germany) as a visiting researcher. Based on his research on functional materials, he designed an energy harvesting device and was granted a patent. He then joined a start-up company to lead a R&D team on energy harvesting technology, and later on joined University of Southampton as a post-doctoral research fellow in 2013. He took up the current post as Lecturer in Energy Harvesting and Storage at Cranfield University in 2016. He has expertise in energy harvesting technologies for applications in environmental sensor network, structural health monitoring and wearable health monitoring. Within this context he has research interest in the development of advanced functional materials and energy harvesting/sensing devices.

Dr. Abiodun Komolafe obtained a BSc (Hons) degree in Physics in 2007 at the University of Ibadan, Nigeria. He obtained an MSc in Microelectromechanical systems in 2011 and in 2016, obtained a PhD in printed circuits on fabrics from the University of Southampton. He is experienced in the fabrication of e-textiles using screen printing and photolithography technologies. He currently works as a Research Fellow in the University of Southampton investigating novel manufacturing methods for making functional electronics on textiles.

Dr Kai Yang received the BSc degree in material engineering from the Beijing Institute of Fashion Technology, China, in 2004 and the PhD degree from the School of Chemistry, University of Leeds, in 2009. She is a Senior Research Fellow in Electronics and Computer Science. Her research interests include electronic textiles, ink formulations, printing, and wearables technologies.

Dr Andrew Robinson received an MEng in Aerospace Engineering at the University of Southampton in 2007, and completed his PhD titled: the assessment of residual stresses using thermoelastic stress analysis, in 2011 also at Southampton. He is now the manager of the Testing and Structures Research Laboratory (TSRL) which is a leading multidisciplinary facility covering a wide range of application areas, specifically specialising in experimental mechanics, structural testing and non-contact imaging techniques.

Dr Russel Torah graduated with a BEng (Hons) in Electronic Engineering in 1999 and an MSc in Instrumentation and Transducers in 2000, both from the University of Southampton. Between 2001 and 2004 Russel obtained a PhD in Electronics from the University of Southampton in the optimisation of thick-film piezoceramics. Since 2005 he has been a full time researcher at the University of Southampton where he is currently a Senior Research Fellow. Dr Torah is a co-founder of the Smart Fabric Inks (in 2011) company specialising in printed smart fabrics. Dr Torah's research interests are currently focused on smart fabric development but he also has extensive knowledge of energy harvesting, sensors and transducers. Dr Torah has 82 publications.

Professor Steve P Beeby obtained a BEng (Hons) degree in Mechanical Engineering from the Univeristy of Portsmouth, UK, in 1992. He obtained his PhD from the University of Southampton, UK, in 1998 on the subject of MEMS resonant sensors. He has been awarded two prestigious EPSRC Research Fellowships to investigate the combination of screen printed active materials with micromachined structures and textiles for energy harvesting. Following the first Fellowship, he became a lecturer in ECS, was appointed a Reader in 2008 and was awarded a personal Chair in 2011. His research interests include energy harvesting, e-textiles, MEMS and active printed materials development. He leads the UK's Energy Harvesting Network and is Chair of the International Steering Committee for the PowerMEMS conference series. He is currently leading 3 UK funded research projects and has previously been principal or co-investigator on a further 18 projects and co-ordinated 2 European Union research projects. He has co-authored/edited four books including 'Energy Harvesting for Autonomous Systems' (Artec House, Inc., Boston, London, 2010). He has given 14 invited talks and has over 200 publications and 10 patents. He has an h-Index of 39 with >9500 citations. He is a co-founder of Perpetuum Ltd, a University spin-out based upon vibration energy harvesting formed in 2004, Smart Fabric Inks Ltd and D4 Technology Ltd.

References:

[1] S. P. Beeby, J. M. Tudor, N. M. White, Meas. Sci. Technol. 17 (2006) R175-R195.
[2] C. R. Bowen, H. A. Kim, P. M. Weaver, S. Dunn, Energy Environ. Sci. 7 (2014) 25-44.
[3] Z. Luo, D. Zhu, J. Shi, S. Beeby, C. Zhang, P. Proynov, B. Stark, IEEE Trans. Dielectr. Electr. Insul. 32, (2015) 1360-1368, 2015.
[4] S. Roundy, P. K. Wright, Smart Mater. and Struct. 13 (2004) 1131-1142.
[5] D. Zhu, S. P. Beeby, M. J. Tudor, N. R. Harris, Sens. and Act. A 169 (2011) 317-325.
[6] X. Wang, Nano Energy 1 (2012) 13-24.
[7] J. Yan, Y. G. Jeong, Appl. Mater. Interfaces (2016) 15700-15709.
[8] R. L. Hadimani, D. V. Bayramol, N. Sion, T. Shah, L. Qian, S. Shi, E. Siores, Smart Mater. Struct. 22 (2014) 075017.
[9] K. S. Ramadan, D. Sameoto, S. Evoy, Smart Mater. Struct. 23 (2014) 033001
[10] T. Papakostas, N. White, Sensor. Rev 20 (2000) 135-139.
[11] K. Prashanthi, N. Miriyala, R. D. Gaikwad, W. Moussa, V. R. Rao, T. Thundat, Nano Energy 2 (2013) 923-932.
[12] T. Bhimasankaram, S. V. Suryanarayana, G. Prasad, Curr. Sci. 74 (1998) 967-976.
[13] E. Sancaktar and L. Bai "Electrically conductive adhesives", Polymers, vol.3, pp.427-466, 2011.
[14] Z. Ounaies, C. Park, J. Harrison, P. Lillehei, J. of Thermoplastic Composite Materials 21 (2008) 393-409.
[15] H. L. Zhang, J-F. Li, B-P. Zhang, J. Electroceram.16 (2006) 413-417.
[16] W-S. Jung, M-J. Lee, S.J. Yoon, W-H. Lee, B-K. Ju, C-Y. Kang, Int. J. Appl. Ceram. Technol. 13 (2016) 480-486.
[17] A. Almusallam[1], R. N. Torah, D. Zhu, M. J. Tudor, S. P. Beeby, J. of Phys.: Conf. Series 476 (2013) 012108.
[18] A. Almusallam, K. Yang, Z. Cao, D. Zhu, M. J. Tudor, S. P. Beeby, J. of Phys.: Conf. Series 557 (2014) 012083.
[19] A. Almusallam, K. Yang, D. Zhu, R. N. Torah, A. Komolafe, J. Tudor, S. P. Beeby, Smart Mater. Struct. 24 (2015)115030.
[20] K. Yang, R. Torah, Y. Wei, S. Beeby, J. Tudor, Textile Research Journal 83 (2013) 2023-2031.
[21] A. O. Komolafe, PhD thesis, Electronics and Computer Science, University of Southampton, 2016.
[22] X. Feng, Y. Huang, A. J. Rosakis, Trans. of the ASME 74 (2007) 1276-1281.
[23] R. G. Ballas, in Piezoelectric muyltilayer beam bending actuators, ed, (2007) 54.

[24] S. Xu, Y.-W. Yeh, G. Poirier, M. C. McAlpine, R. A. Register, N. Yao, Nano Lett. 13 (2013) 2393−2398.
[25] B. K. Yun, Y. K. Park, M. Lee, N. Lee, W. Jo, S. Lee, et al., Nanoscale Res. Lett. 9 (2014) 4.
[26] K.-I. Park, M. Lee, Y. Liu, S. Moon, G.-T. Hwang, G. Zhu, et al., Adv. Mat. 24 (2012) 2999–3004.